International Journal of Hydrogen Energy 263 (2026) 156784

Contents lists available at ScienceDirect

International Journal of Hydrogen Energy

journal homepage: www.elsevier.com/locate/he

Pioneering underground hydrogen storage: Insights from a first-of-its-kind field demonstrator in a depleted gas reservoir

Anitha Andiappan [a,*], Franziska Steger [a], Aleksander Makaruk [b], Artur Zaduryan [c], Katarina Nieke [a], Benedikt Hasibar [a], Andreas P. Loibner [c], Markus Pichler [a], Stephan Bauer [a]

[a] RAG Austria AG, Vienna, Austria
[b] Axiom Angewandte Prozesstechnik GmbH, Ebreichsdorf, Austria
[c] Institute of Environmental Biotechnology, Department of Agrobiotechnology IFA-Tulln, BOKU, University of Natural Resources and Life Sciences, Vienna, Austria

ARTICLE INFO

Keywords:
Underground hydrogen storage
Depleted gas reservoir
Field application
Technical feasibility
Operational safety
Integrated system

ABSTRACT

Underground hydrogen storage (UHS) is a key enabler of the hydrogen economy, providing large-scale, long-term energy storage and supporting industrial decarbonization. Depleted porous reservoirs offer a promising option, although concerns about reservoir integrity, hydrogen-rock or -fluid reactions, and microbial activity have delayed deployment. Over a decade, extensive studies and field tests have addressed these challenges. The consistently positive results enabled RAG Austria AG to develop the first demonstrator-scale pure hydrogen storage facility in a depleted gas reservoir integrated into the local energy network. This article presents results from two successful storage cycles achieving 450,000 Nm^3 of stored hydrogen and recovered purity above 98 vol% prior to conditioning. H_2S remained below detection limit, indicating negligible souring. Reservoir surveillance showed behaviour comparable to natural gas storage, confirming technical feasibility and safety. These findings reduce technical barriers, increase the Technical Readiness Level (TRL), and support UHS as a cornerstone of future energy systems.

1. Introduction

The global shift from fossil fuels to renewable energy sources such as solar and wind is increasingly evident in contemporary energy systems [1]. However, this transition introduces a significant challenge: intermittency, as renewable energy generation is not consistently aligned with demand. To address this, substantial energy storage capacity is required beyond the short-term solutions currently available in the electricity grid, such as batteries and pumped hydropower. Large-scale energy-storage enables both short-term balancing and seasonal energy management, ensuring a stable and reliable energy supply [2].

Hydrogen (H_2), particularly green H_2 produced via electrolysis using renewable electricity, emerges as a promising and flexible energy carrier [3]. It enables the storage of surplus renewable energy for later use and serves as a critical feedstock for hard-to-abate sectors, especially the chemical industry, where H_2 can substitute natural gas in essential processes [3]. Consequently, large-scale storage is indispensable to ensure a secure and continuous supply across these industries and the broader energy system. One viable approach is to store H_2 in naturally occurring porous subsurface formations, which offer significantly greater storage capacity than surface-based alternatives. Several studies have demonstrated that underground hydrogen storage (UHS) provides economic advantages, including reduced land use, enhanced scalability, and lower surface-level risks compared to aboveground systems [4,5].

Looking ahead, UHS is expected to play a critical role by 2050 in bridging the gap between H_2 production and consumption, particularly for seasonal and long-term energy balancing needs [6]. Recognizing its strategic importance, several European countries like Austria, Germany, the Netherlands, France and the UK have included UHS into their national energy roadmaps [7–12]. Various geological formations are suitable for UHS, similar to those used for natural gas storage. An overview can be found in Table 1.

Today, salt caverns account for roughly 26% of global gas storage deliverability yet represent only a small fraction of total working gas capacity. In contrast, depleted gas reservoirs dominate underground gas storage worldwide, providing approximately 80% of global working gas capacity [15]. Since H_2 has only one-third of the volumetric energy density of natural gas, future energy systems will require much larger storage volumes, estimated at 300 TWh in the EU by 2050 [16,17]. Given their widespread availability, large storage potential, and opportunities for infrastructure reuse, depleted gas reservoirs stand out as one of the most promising options for UHS. Building on this context, this paper focuses specifically on UHS in a depleted gas reservoir.

* Corresponding author.
E-mail address: anitha.andiappan@rag-austria.at (A. Andiappan).

https://doi.org/10.1016/j.ijhydene.2026.156784
Received 20 February 2026; Received in revised form 10 July 2026; Accepted 24 July 2026
Available online 31 July 2026

Table 1
Overview of geological formations that are suitable for UHS.

Geological formation	Description	Capacity scale	Key advantages	Limitations	Typical use case
Salt Caverns [13]	Solution-mined cavities in salt formations	GWh (short duration: weeks–months)	Very high deliverability; fast injection and withdrawal	Geographically limited; low total capacity	Peak shaving; short-term balancing; Dunkelflaute mitigation
Depleted Gas Reservoirs [12]	Porous reservoir rock with sealing caprock, previously used for gas extraction	TWh (large-scale, seasonal)	Very high storage capacity; existing infrastructure; well understood	Slower deliverability compared to salt caverns	Seasonal storage; strategic reserves
Saline Aquifers [14]	Porous rock formations filled with brine	Large theoretical potential (not widely commercialized)	Vast potential storage volume	Limited subsurface data; need for significant cushion gas volumes; pressure management challenges; absence of existing infrastructure	Not widely used

The challenges of UHS in porous reservoirs have been increasingly recognized over the past decade [18]. Key concerns included geochemical stability of reservoir and cap rocks, microbial activity and possible byproducts, leakage risks due to hydrogen's small molecular size, and uncertainties in transport behaviour. Since then, extensive laboratory, theoretical, and field investigations have been conducted to evaluate feasibility, integrity, and safety. Results from major projects such as Hystories [19] HyStorPor [20], HyUSPRe [21], Underground Sun Storage [22], Underground Sun Conversion [23] consistently suggest that no fundamental barriers have been identified under the investigated conditions, supporting the feasibility of implementation. Caprock experiments demonstrated long-term sealing integrity under H_2 exposure, with no measurable changes in mineralogy, porosity, or permeability after one year at representative pressure and temperature [24]. Similarly, RAG's sandstone reservoir samples subjected to H_2-rich mixtures (up to 75 vol%) and pure H_2 at 200 barg showed no alteration in porosity or mineral composition, confirming reservoir rock stability [25]. Transport studies revealed H_2 diffusivity in porous media to be low (10^{-7}–10^{-9} m^2/s), indicating that diffusion plays only a minor role compared to pressure-driven flow [26]. Dispersion experiments further confirmed homogeneous distribution of H_2, with negligible adsorption effects [27].

Recent studies also investigated the relevance of microbiology in UHS [28–30]. Microbial activity can lead to localized H_2 consumption through processes such as hydrogenotrophic methanogenesis ($4\ H_2 + HCO_3^- + H^+ \rightarrow CH_4 + 3\ H_2O$, −135.6 kJ/mol) and sulphate reduction ($4\ H_2 + SO_4^{2-} + H^+ \rightarrow HS^- + 4\ H_2O$, −151.9 kJ/mol), producing only minor by-products. Despite being thermodynamically favourable, overall H_2 consumption remains low [28,31,32]. Experimental and field investigations typically indicate no adverse effects on reservoir integrity or storage performance [29]. Observed by-products, such as hydrogen sulfide (H_2S), remain below safety thresholds and can be managed effectively through monitoring [28].

Field-scale experience has been gained by RAG Austria AG at the Lehen site, where natural gas containing up to 20 vol% of H_2 has been injected and withdrawn from a porous sandstone reservoir since 2016. Reservoir permeability remained substantially stable, with H_2 behaviour comparable to conventional natural gas storage [22,33]. Minor H_2S formation was observed during withdrawal cycles but consistently remained below regulatory limits [26]. These findings, together with previous laboratory and pilot scale studies, demonstrate the technical feasibility of largescale H_2 storage in depleted gas reservoirs and provide a robust foundation for the demonstration tests presented in this publication.

As H_2 becomes increasingly integrated into energy systems, attention must extend beyond subsurface storage to the recovery processes that ensure its effective reintegration into the energy value chain. In this regard a critical aspect is the conditioning of the withdrawn gas, which mixes to some extend with residual natural gas or other reservoir derived impurities. Withdrawn H_2 typically contains methane (CH_4) as the dominant impurity, along with C_2+ hydrocarbons, carbon dioxide (CO_2), and traces of nitrogen (N_2), as well as organic and inorganic sulfur components, and water vapour. Spatial heterogeneity within the reservoir leads to temporal variations in impurity levels during withdrawal, posing additional challenges for purification.

Hydrogen off-takers and grid operators, however, require consistent and standardized H_2 quality. According to ISO 14687:2025 standard [34], H_2 purity requirements vary by application. H_2 transportation via pipelines generally requires ≥98% purity, with discussions in some regions moving towards 99.5% [35]. Fuel cells demand even stricter specifications, whereas internal combustion engines tolerate lower H_2 concentrations but still impose tight limits on combustible impurities due to their influence on combustion behaviour [34]. These constraints highlight the need for robust and flexible purification technologies capable of meeting stringent quality standards under dynamically changing withdrawal conditions.

Furthermore, the implemented UHS demonstrator can operate in a seasonal manner reflecting the need of renewable energy storage. It realizes the seasonal energy shift by generating renewable H_2 from abundant summer energy and releasing it as pure H_2 during the energy shortage in winter months.

Although current studies indicate that porous reservoirs in the Molasse Basin are suitable candidates for UHS and operate analogously to natural gas storage, these findings are largely based on laboratory investigations, modelling studies, or pilot-scale field tests. In particular, the feasibility and safety of storing pure H_2 in depleted gas reservoirs under fully integrated industrial-scale conditions, followed by withdrawal and end use, have not yet been demonstrated. In addition, the variability in gas composition during withdrawal and the need to meet strict hydrogen purity requirements introduce operational challenges that have not yet been sufficiently addressed in previous studies. This represents a critical gap in establishing a complete hydrogen value chain and limits the large-scale deployment of UHS as a reliable energy solution. To address this gap, the objective of this study is to evaluate the technical feasibility, operational performance, and hydrogen quality management of a fully integrated pure-hydrogen storage system in a depleted gas reservoir under real operating conditions.

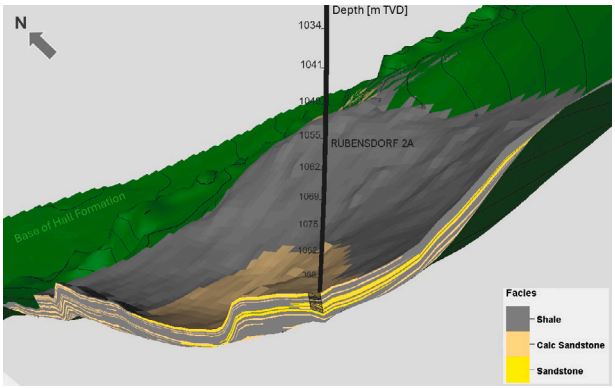

Fig. 1. Facies map in 3D model showing active well Rubensdorf 2 A.

Table 2
Reservoir parameters of UHS Rubensdorf.

Parameter	Unit	Demonstrator
Field	–	UHS Rubensdorf
Depth	m TVD below mean sea level	528
Depth	m TVD below surface	1100
Formation thickness	m	2
Rock formation	–	Hall Series
Rock type	–	Sandstone
Porosity	%	7–17
Permeability	mD	5–95
Water saturation	%	40
Static pressure range	bar(a)	22–107
Storage volume – H_2	million Nm^3	~1
Injection rate	$Nm^3\ h^{-1}$	400
Withdrawal rate	$Nm^3\ h^{-1}$	400–600
Storage wells	#	1
Monitoring wells	#	1

The present study reports the results from the world's first large-scale demonstrator of pure hydrogen storage in a depleted reservoir of the Austrian Molasse Basin. By integrating storage, withdrawal, gas conditioning, and end use within a single operational system, the study demonstrates TRL 7 and provides a comprehensive assessment of UHS performance under real operating conditions.

2. Material and methods

2.1. Demonstrator site

The demonstrator site was developed to validate the technical feasibility and safe storage of H_2 in porous rock formations under real in-situ conditions. The site was selected due to its relatively small size and isolation from neighbouring fields, which minimized external geological influences and operational interference. This setting allowed for clearer interpretation of cause–effect relationships and more controlled experimental conditions.

2.1.1. Geological setting and reservoir characteristics

The Rubensdorf demonstrator site in Upper Austria, Austria utilizes a depleted Eggenburgian gas reservoir, deposited in a turbidite fan pattern (Fig. 1). The thin-bedded reservoir sandstones originate from a conduit in the Southern Imbricates with deposition along the Alpine thrust front, commonly referred to as the "South Slope Play" in internal and external studies [36]. The Eggenburgian reservoir and its intraformational clay-rich caprocks are well-documented [37–39], providing a reliable trap through both sealing capacity and structural configuration as indicated by historical drilling observations. The following Table 2 presents the parameters of the Rubensdorf reservoir.

2.1.2. Cushion gas to working gas ratio

The reservoir was operated with a cushion-to-working gas ratio of approximately 60:40. Residual natural gas from previous production of 0.25 Mio Nm^3 contributed to the cushion gas, which was supplemented to achieve the required pressure support for storage operations. For a planned working gas volume of 1 million Nm^3, a total cushion gas volume of approximately 1.5 million Nm^3 was required.

2.1.3. Well integrity

The reservoir has a single active well, Rubensdorf 2 A, which is used for both injection and withdrawal as well as monitoring. The absence of legacy wells in the reservoir significantly reduced the risk of leakage pathways, thereby enhancing system integrity and simplifying monitoring activities. The undisturbed subsurface environment is particularly advantageous for experimental hydrogen storage, ensuring reliable containment and consequently simplifying permitting processes.

2.2. Operational setup

2.2.1. Field preparation

In addition to the 0.25 million Nm^3 of natural gas present in the reservoir, 0.75 million Nm^3 of natural gas was injected to provide sufficient pressure support for UHS operations. The well completion was modified to meet both conventional storage requirements and hydrogen service conditions, including the installation of a surface-controlled subsurface safety valve (SSSV; Halliburton NE^{TM} Tubing-Retrievable Safety Valve PN 478LXA21-CAC) and L80-grade standard NG steel tubing (according to API 5CT), which has been positively tested for H_2 compatibility [40]. Following these modifications, the remaining cushion gas of approximately 0.5 million Nm^3 was injected as H_2 to prepare the system for hydrogen storage operation.

2.2.2. Surface facility setup

To realize UHS in the Rubensdorf reservoir, an above-ground facility was designed and constructed in accordance with established process engineering practices. A simplified process scheme of the surface installation is shown in Fig. 2. The surface units largely corresponded to those of conventional natural gas storage facilities, with additional components required for seasonal UHS: an electrolyzer, an adapted gas purification unit and dedicated gas analysis system.

H_2 was generated on site using a proton exchange membrane electrolyzer (ACCELERA by CUMMINS; HyLYZER 400) with a rated power of 2 MWe and a nominal output of 400 Nm^3/h at the pressure of 26 to 30 barg. The product H_2 was deoxidated, dried and subsequently directed to the compressor system (depicted as 1st compressor in Fig. 2) comprising of two parallel, gastight, electrically driven, two-stage piston compressor units (HAUG; SIRIUS 42G). Their primary function was to enable reservoir injection at pressures up to 70 barg during the storage season. In addition, the compressors were operated during the hydrogen withdrawal to boost low storage pressures and allow pipeline injection. The compressed H_2 was directly injected into the reservoir through the Rubensdorf 2 A well at rates up to 400 Nm^3/h. To ensure operational flexibility, H_2 was injected from a trailer supply whenever the electrolyzer was unavailable.

During withdrawal, H_2 was produced at rates of up to 600 Nm^3/h. Before entering the H_2 pipeline, the withdrawn gas underwent multistep conditioning. First, the well stream is routed to a free water knockout vessel (OTTO KLEIN; OKZA 300) comprising a fully welded upright cyclone separator to remove entrained solids and liquids.

The next conditioning step was gas dehydration, performed using a fixed-bed Temperature Swing Adsorption (TSA) unit (SILICA; SILDRY TA/TT) composed of two molecular sieve adsorbers operated alternately in adsorption and regeneration modes. During regeneration, desorbed vapour was condensed and removed from the unit. Liquids

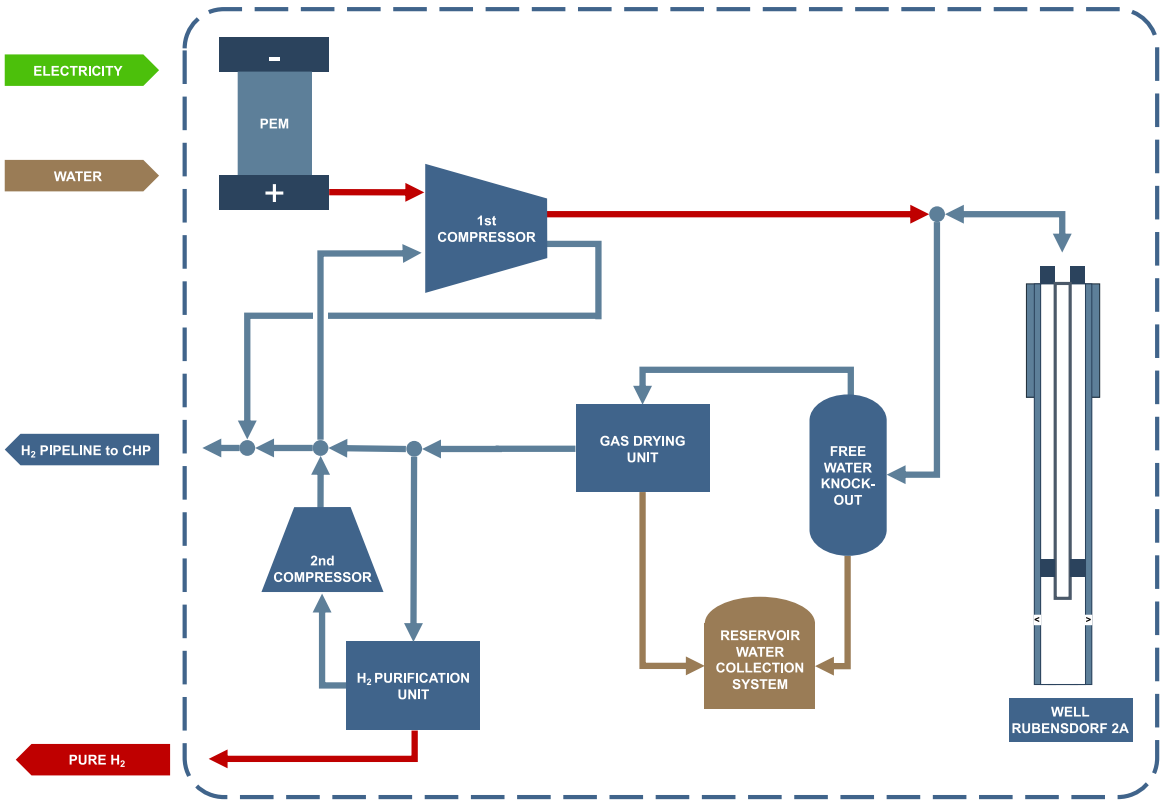

Fig. 2. Surface facility schematic of UHS Rubensdorf.

from both the knockout vessel and the TSA system were collected in a tank and transported offsite.

Following the dehydration step, a portion of the withdrawn gas was directed into a dedicated hydrogen purification unit. This High-Pressure Swing Adsorption (HPSA) system removed residual impurities originating from the natural gas cushion gas. The HPSA unit comprised four adsorbers filled with high strength activated carbon granulate capable of broadband separation of natural gas constituents from H_2. It was designed for operation at pressures up to 75 barg, was capable of processing the gas flow up to 180 Nm^3/h. A detailed laboratory investigation of the applied adsorbent is reported elsewhere [41]. Because the unit is driven directly by the wellhead pressure, its operating pressure declines along with the decreasing reservoir pressure. To accommodate variable UHS operating conditions, which are reflected in declining feed gas pressures and time dependent hydrogen–natural gas mixture compositions, a proactive control strategy with variable valve timing and an optimized PSA cycle was employed in the unit. Selected aspects of HPSA operation under variable storage conditions are discussed in the process simulation study by Kalman et al. (2024) [42].

Pure H_2 could be withdrawn directly from a dedicated HPSA product outlet as shown schematically in Fig. 2. The remaining uncollected withdrawn H_2 was mixed with the HPSA tail gas, after its pressure was augmented with the HPSA-integrated piston compressor (shown as 2nd Compressor in Fig. 2). The resulting gas mixture was transported via an eight-kilometre long pipeline to a Combined Heat and Power (CHP) unit for local electricity and heat production. Alternatively, the site was also equipped to blend the withdrawn H_2 into the public natural gas grid, however this pathway was used to a very limited extent during the site operations.

2.3. Reservoir monitoring

2.3.1. Surface measurements at wellhead

The flow rates of both injected and produced gas were continuously measured using an Emerson CMFS040 flowmeter, which offers a precision of +/− 0.1%. In addition, the gas composition of the injected and produced streams was continuously (cycle time = 4 min) monitored via an Emerson 700XA gas chromatograph, with a precision of +/− 0.3 Vol %, enabling the analysis of major components such as H_2 and CH_4, as well as secondary components (C_2H_6, CO_2, and H_2S), particularly during withdrawal phase prior to gas conditioning.

Tubing head pressure (THP) and surface temperature were also monitored continuously with an Emerson 3051TG4 sensor and an E&H PMP 51B EDGE Speaker, respectively. Furthermore, annular pressures between the casing and tubing, as well as between concentric casing strings, were continuously monitored using pressure gauges. Additional verification of tubing-casing annulus pressure was provided by the MURAG 20 (RAGSOL; EDGE SPEAKER), an acoustic-based measurement system that calculates subsurface pressure from liquid level monitoring in the annulus [43,44]. MURAG 20 enables continuous automated monitoring under dynamic operating conditions.

2.3.2. Surface measurements at the gas purification unit

The assessment of the HPSA system performance relied on a laser methane residual content measurement with a detection limit of approximately 1 ppm in the purified H_2. Mass stream balances were determined from measured mass flows of the relevant streams, i.e. feed, product gas and tail gas, using the Coriolis method. In addition, the unit was equipped with pressure and temperature transmitters at key process points to support system analysis and ensure safe operation.

2.3.3. Downhole measurements of pressure and temperature

Downhole pressure and temperature were continuously monitored using quartz gauges (Shortline-EM Piezo Memory Gauge; Reservoir Group) installed within the well tubing, near the perforation zone. To ensure data reliability and redundancy, two quartz gauges were mounted in parallel.

Pressure transient tests were conducted throughout the lifetime of the Rubensdorf 2 A well, including buildup periods following injection shut-ins and falloff tests after withdrawal phases. These data were evaluated using a consistent pressure transient analysis (PTA) workflow. Raw pressure data were quality-controlled, including drift correction, removal of operational disturbances, and cross validation between gauges.

Analysis was performed using derivative based interpretation, combining Horner diagnostics and log–log pressure derivative plots to identify flow regimes. Model matching was carried out using a radial flow analytical model under single phase gas assumptions, applied uniformly to natural gas, N_2, and H_2 test periods. Key parameters such as permeability and stabilized reservoir pressure were estimated, and boundary conditions were assessed where data allowed. All PTA evaluations were conducted using the Ecrin KAPPA 5.6 software suite with consistent modelling assumptions to enable comparison of reservoir behaviour over time.

2.3.4. Laboratory analysis of gas samples at wellhead and gas purification unit

To verify the gas chromatograph measurements, additional gas samples were periodically collected from the production tubing and analysed by a certified laboratory. Furthermore, vent gas sampling was conducted in the annular space between the casing and tubing (Annulus A) and analysed by a certified laboratory. These samples were typically taken at the highest and lowest storage levels to assess barrier integrity, detect potential gas intrusion, and identify possible gas migration.

To confirm the purity of the H_2 product from the HPSA unit, a comprehensive component analysis was performed, following DIN 51872. During operation, product gas was sampled in stainless steel cylinders and analysed using laboratory gas chromatography. The analysed components included oxygen, N_2, CO_2, CH_4, ethane, propane, isobutane, n-butane, isopentane, n-pentane, and nC_6+ (reported as a lumped fraction). A limitation of the applied method is the relatively high DL of 100 ppm for the measured components. The H_2 index in the HPSA hydrogen product gas was measured by the selective laser beam absorption device.

2.3.5. Sampling and laboratory analyses of subsurface brine

Subsurface brine samples were collected from the production well sump using a downhole sampler following the protocol of Hellerschmied et al. (2024) [45]. The sampler was sterilized and deployed to the perforated interval of the gas-bearing sandstone. After retrieval, samples were transferred to autoclaved, gas-tight glass bottles and purged with high-purity argon to establish an oxygen-free atmosphere. Samples were stored in the dark at <8 °C until processing within 12 h.

Subsequent laboratory analyses followed the procedures described by Hellerschmied et al. (2024) [45]. Brine aliquots were handled under anoxic conditions for physicochemical and molecular characterization. Microbial biomass was recovered by centrifugation and filtration, followed by DNA extraction (FastDNA SPIN DNA extraction Kit, MP Biomedicals, USA) using a standard protocol with the following modifications: the homogenization in the FastPrep-24 homogenizer unit was performed 4 times for 60s at 5.5 m/s.

Subsequently, sequencing and bioinformatic analyses were performed. The V4 region of the 16S rRNA gene was amplified and sequenced with 515f [46] and 806r [47] primer pair by Microsynth AG Switzerland (MiSeq platform, 2x250 bp). Sequence analysis including primer removal, quality filtering, denoising, paired-end merging, chimera removal, amplicon sequence variant (ASV) inference, and taxonomic classification against the SILVA 138.2 database [48] as well as downstream analysis were done with an in-house DADA2-based [49] bioinformatics pipeline. ASVs were grouped by genus, and genera with relative abundance below 2% were collapsed into "Other" in Fig. 6. Functional assignments were performed with FAPROTAX [50].

3. Results and discussion

3.1. Implementation of the proposed UHS system

3.1.1. Overview of the implementation

As outlined in the Materials and Methods Section 2.2.1, the Rubensdorf reservoir was prepared for UHS through staged cushion gas injection and infrastructure upgrades completed by July 2023. Fig. 3 depicts the evolution of gas volumes in the reservoir over time, with cushion gas represented below the zero line and working gas above. The orange-shaded region indicates the initial 1 million Nm^3 of natural gas used as cushion gas, which maintained a stable reservoir pressure of 37 bara.

Following the well's repurposing for hydrogen service in February 2024, an additional 0.5 million Nm^3 of H_2 was injected, raising the pressure to 46 bara and completing the cushion gas volume.

In principle, optimal H_2 recovery during withdrawal is achieved when the cushion gas consists entirely of H_2. However, a mixed cushion gas strategy was adopted due to the limited temporal availability of H_2 and to reflect conditions typical of converting existing natural gas storage facilities to UHS. Consequently, approximately one third of the cushion gas volume consisted of H_2. The green-shaded region above the zero line in Fig. 3 represents the working gas volume (WGV), which displays two distinct storage cycles. The first, a smaller cycle from March to June 2024, reached a peak H_2 volume of approximately 75,000 Nm^3. The second, larger cycle began in August 2024 and extended through May 2025, achieving a maximum storage volume of 450,000 Nm^3 of H_2.

Throughout these operations, the tubing head flowing pressure envelope ranged between 30 and 70 barg. H_2 was injected at a rate of approximately 400 Nm^3/h. During withdrawal a rate of up to 600 Nm^3/h was produced, depending on the intake rate of the CHP unit. This demonstrates that hydrogen can be handled operationally in a manner consistent with established natural gas storage practices, indicating strong potential for repurposing existing infrastructure for UHS with minimal adaptation.

3.1.2. First storage cycle

The first cycle served as a test phase that commenced between March to June 2024, during which only a small volume of working gas was injected. The primary objective was to assess whether the surface setup functioned as intended and to identify any potential operational issues. Fig. 4A illustrates the concentration profiles of the main components, specifically H_2, and CH_4 (CH_4) in the withdrawn gas stream over time. The concentration profiles of H_2 reduced by 0.2 vol% and CH_4 increased by 0.2 vol% gradually over time.

In this cycle, C_2H_6 (Fig. 4C) remained below the DL except for an outlier on 25 June 2024, while the CO_2 concentration (Fig. 4C) increased gradually to a maximum of 40 ppm at the end of the first withdrawal cycle. As shown in Fig. 4E, the concentration of H_2S was also monitored and remained consistently below the DL of 0.20 ppm of the installed gas chromatograph throughout the first withdrawal cycle. An interruption in the data record between 22 June 2024 and 25 June 2024 is visible in Fig. 4A, Fig. 4C and Fig. 4E during the first withdrawal cycle. This gap resulted from the temporary shutdown of the CHP unit, which served as the hydrogen off-taker. As the CHP was not in operation during this period, no H_2 was withdrawn from the reservoir.

To validate the measurements obtained from the gas chromatograph, a gas sample was collected on 19 June 2024 and analysed by a certified laboratory. The results (see Supplementary Material A)

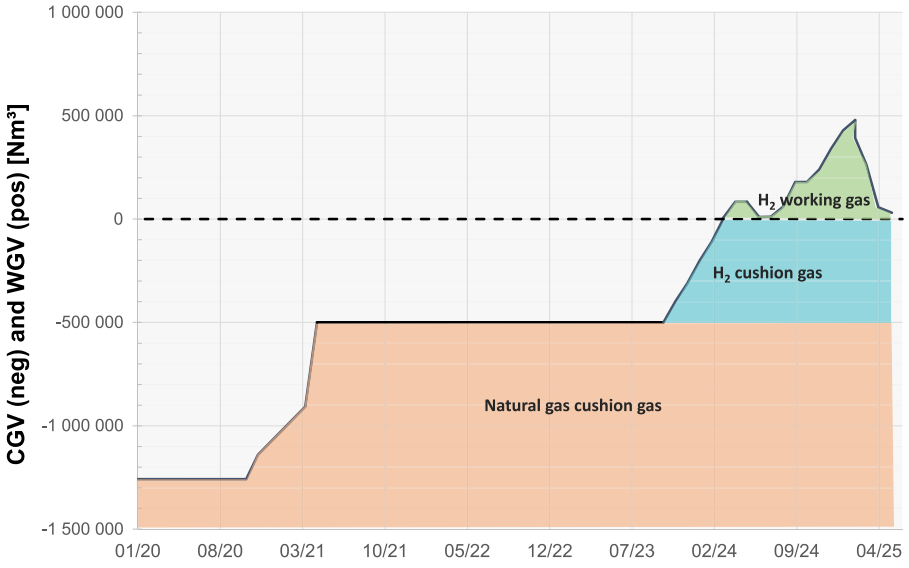

Fig. 3. Storage level in Rubensdorf reservoir including timeline of cushion gas injection.

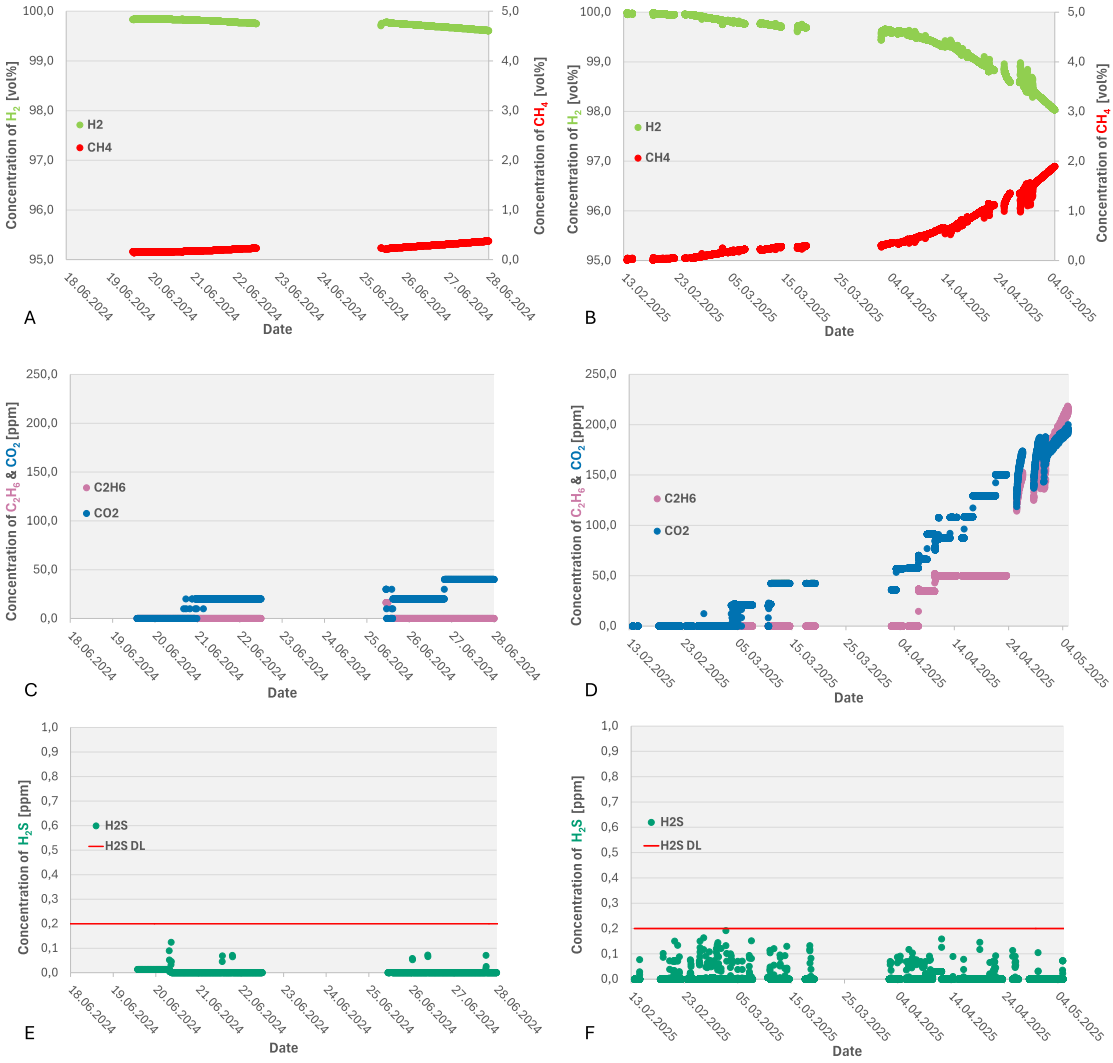

Fig. 4. Gas composition over time during withdrawal phase in 1st cycle (left) and 2nd cycle (right). H_2 and CH_4 recoveries in 1st cycle (A) and 2nd cycle (B). Ethane (C_2H_6) and CO_2 concentrations in 1st cycle (C) and 2nd cycle (D). H_2S concentrations in 1st cycle (E) and 2nd cycle (F).

confirmed the accuracy of the chromatographic analysis. Furthermore, a gas sample from Annulus A (between the tubing and casing) taken on 21 February 2024 revealed trace levels of H_2 (0.06 vol%), after approximately 400,000 Nm^3 of H_2 had been injected as cushion gas into the reservoir (see Supplementary Materials B). This indicates that the H_2 remains confined within the tubing, suggesting the well completion is intact.

The gas concentration profiles (Fig. 4A) show a gradual decrease in H_2 and a corresponding increase in CH_4 over time. The detected CH_4 concentrations remained far below those present in the original cushion gas composition (see Supplementary Materials C) reflecting that the withdrawn gas originated predominantly from the H_2 working gas volume, as expected. This behaviour is consistent with a reported reservoir-scale dilution effect [51] and reflects controlled mixing between injected hydrogen and residual cushion gas. The stability of these trends indicates consistent withdrawal dynamics and absence of unexpected compositional shifts, supporting the suitability of the Rubensdorf reservoir for UHS, which is essential for maintaining hydrogen recovery efficiency and gas quality in UHS systems. Ethane concentrations remained below the DL, likely because only limited gas volumes were withdrawn during the first cycle and the well did not produce sufficient gas volumes from the deeper reservoir sections. The apparent outlier is most plausibly an artefact associated with production resuming after a shut-in period. The detected CO_2 concentrations, which are far below those in the original cushion gas, can be explained by reservoir scale dilution and transport processes. Although the cushion gas initially contained approximately 0.1 vol% CO_2 (see Supplementary Materials C), subsequent H_2 injection greatly increased the total gas volume, dispersing and diluting the CO_2 within the much larger H_2 dominated working gas volume. Consequently, the withdrawal phase reflects this mixed and highly diluted gas, resulting in CO_2 levels well below the original cushion gas concentration. Although the CO_2/CH_4 ratio in the produced gas appears much higher than in the original cushion gas, this ratio cannot be directly compared. When production begins and reservoir pressure decreases, dissolved CO_2 exsolves rapidly from the reservoir brine and migrates towards the wellbore much faster than CH_4 [52]. As a result, the proportion of CO_2 to CH_4 is relative.

Additionally, H_2S remained below DL and well within the ISO 14687:2025 Grade A limit of 7 ppm [34], indicating high gas purity and providing no evidence of souring during this phase of operation. Owing to the tight commissioning schedule of the overall storage facility, the HPSA unit remained offline throughout the first withdrawal cycle.

The successful execution of the first cycle of pure H_2 injection and withdrawal, despite the minimal gas volumes involved, confirmed that the surface setup functioned as intended. The near absence of operational issues or showstoppers validates the system's implementation and indicates readiness for larger-scale operations.

3.1.3. Second storage cycle

The second cycle involved a substantially larger volume of H_2 of approximately 450 000 Nm^3, injected and withdrawn between August 2024 and May 2025. The temporal evolution of H_2 and CH_4, as well as secondary components such as C_2H_6, CO_2, and H_2S were again monitored throughout the second storage cycle (Fig. 4B, D and F). The H_2 concentration declined more steeply over time compared with the first cycle. However, the final concentration after the complete withdrawal remained high at 98.0 vol%, meeting the minimum hydrogen index defined by ISO 14687:2025 Grade A specification for H_2 content in pipeline transport [34]. The residual gas consisted primarily of CH_4, which increased to a maximum of 1.94 vol% (Fig. 4B), 215 ppm for C_2H_6 (exceeding the ISO 14687 Grade A specification by 115 pm) and 194 ppm CO_2 (H_2D). H_2S (Fig. 4F) remained below DL of the gas chromatograph, consistent with observations from the first withdrawal phase. An interruption occurs in the data record between 19 March 2025 and 2 April 2025 during the second cycle (Fig. 4B, D and F). This was due to the commissioning of the refurbished electrolysis unit, along with maintenance work on other components at the surface facility. In addition, service and troubleshooting activities were carried out on the CHP unit.

To verify the accuracy of the onsite gas chromatograph, two independent sampling campaigns were conducted at the wellhead on 12 March 2025 (see Supplementary Materials D) and 5 May 2025 (see Supplementary Materials E). Both confirmed the reliability of the chromatograph measurements at the Rubensdorf demonstrator site.

During the second withdrawal cycle, the H_2 purification unit was operated along with other gas conditioning surface facilities to evaluate its performance under field conditions. After optimization of the pressure cycle timings, the unit proved to consistently maintain CH_4 concentrations below 100 ppm in the product gas, averaging at 56 ppm for the whole withdrawal period. The achieved average H_2 recovery of HPSA in the cycle equalled 70%, and its variation depended mainly on the CH_4 content and reservoir pressure. The operation of surface facility demonstrated that variations in feed gas composition, inherent to UHS operation, can be effectively managed by an adapted PSA system, enabling consistent delivery of high-purity hydrogen despite dynamic reservoir conditions. Concentrations of C_2+ hydrocarbons, nitrogen, oxygen, and CO_2 in the purified H_2 that were measured by ex-situ GC remained below 100 ppm. The H_2 index confirmed by the precise laser to exceed values of 99.99%. Although the chromatographic detection limit was far from allowing the verification of 1 ppm threshold for C_2+ hydrocarbons, their very low concentrations in the raw withdrawn gas and the high selectivity of the HPSA activated carbon indicate that compliance with this limit can be presumed.

The larger injected H_2 volume in the second cycle provided deeper insight into the reservoir's dynamic behaviour under more representative operational conditions. The steeper decline in H_2 concentration relative to the first cycle is expected to be the consequence of the larger injected hydrogen volume and the associated increase in residence time within the reservoir. The extended storage period strengthened mixing effects such as dispersion and diffusion that acted over longer timescales and across a larger reservoir volume, resulting in a broader mixing zone between hydrogen and residual cushion gas [53,54]. Despite the steeper increase in methane concentration during withdrawal, the final H_2 concentration remained above 98.0 vol% (Fig. 4B) . This underscores the suitability and robustness of the reservoir for large-scale underground H_2 storage under more representative storage volumes and operating conditions.

The gradual increase in CH_4 concentration to 1.94 vol% (Fig. 4B) may reflect the presence of residual gas from previous operations. Owing to reservoir-scale dilution, and although CH_4 concentrations in the second cycle were higher than in the first, these values remain far below those of the original cushion gas composition (see Supplementary Materials C). This indicates that the withdrawn gas originated predominantly from the H_2 working gas volume, consistent with the behaviour observed during the first cycle's withdrawal phase. This confirms that mixing with cushion gas remains limited and predictable, which is essential for maintaining hydrogen recovery efficiency during repeated storage cycles.

According to Fig. 4D, C_2H_6 and CO_2 concentrations were more pronounced in the second withdrawal cycle, reflecting the larger hydrogen volume injected and the associated increase in residence time and reservoir contact. This behaviour is consistent with enhanced reservoir-scale mixing discussed above [53]. During withdrawal, CO_2 concentrations were initially higher than those of C_2H_6, whereas towards the end of the cycle C_2H_6 exceeded CO_2. Although C_2H_6 is lighter and more diffusive, CO_2 appeared earlier at the wellhead, primarily due to its higher solubility in formation water. As reservoir pressure decreases during production, dissolved CO_2 exsolves rapidly and is transported towards the wellbore, leading to an early CO_2 peak despite its lower mobility compared to ethane [55,56]. Towards the end of the withdrawal cycle, C_2H_6 became dominant, likely due to its higher concentration in the

Table 3
PTA interpretation over the lifetime of well Rubensdorf 2 A.

Date	Test	Netto [TV Dss m]	Avg. Porosity [%]	Permeability [mD]	Medium
2013	Cased Hole Test	1.18	16	51	Natural Gas
2020	Injection Fall-Off Test	1.18	16	59	N_2
2021	Fall-Off Test	1.18	16	68	Natural Gas
2025	Build-Up Test	1.18	16	63	H_2

cushion gas and its release from regions further away from the wellbore as the withdrawal front progressed (see Supplementary Materials C).

These observations lead to the conclusion that compositional evolution during hydrogen withdrawal is governed by the combined effects of thermodynamics (gas solubility), reservoir heterogeneity, and transport processes. Importantly, the increasing contribution of these components with larger storage volumes highlights the need to account for time-dependent mixing processes when predicting gas quality and designing UHS operations.

Once again, the persistent H_2S levels below the DL throughout the second cycle provide strong indication of chemical and microbiological stability, as well as favourable geochemical conditions that suppress souring. This is particularly significant, as even low levels of H_2S can impact material integrity, gas quality, and surface processing requirements, making its absence a key indicator of reservoir suitability for repeated hydrogen storage cycles.

The validated performance of the gas chromatograph strengthens confidence in the reported concentration trends and confirms the robustness of the monitoring framework applied in the demonstrator project [57]. The HPSA results further demonstrate that the purification system can reliably produce H_2 suitable for fuel-cell applications, even under varying feed-gas compositions.

In summary, the second storage cycle confirmed that the reservoir can accommodate larger H_2 volumes while maintaining gas integrity, operational safety, and predictable compositional behaviour under the investigated conditions. Furthermore, the second cycle illustrated the system's capability for seasonal operation, with surplus summer energy stored as H_2 and subsequently withdrawn during the winter demand period (February–May 2025). These results highlight the potential of depleted gas reservoirs to serve as scalable and flexible components of future hydrogen systems, supporting both grid balancing and long-term energy storage.

3.2. Downhole monitoring and numerical analyses

The subsurface pressure data were further evaluated using PTA which interprets pressure responses following well operations to estimate reservoir permeability, identify boundary conditions, and characterize flow regimes. Multiple PTA evaluations were conducted on the Rubensdorf 2 A well, based on build-up and fall-off tests performed throughout the lifetime of the well, as summarized in Table 3. This approach enables a quantitative basis for assessing reservoir integrity over time and enabling direct evaluation of the impact of hydrogen injection on reservoir performance.

The analyses indicate that reservoir permeability remained stable over time, consistently ranging between 50 and 70 millidarcies (mD). The use of N_2 during a suitability test in 2020 was based solely on availability and had no technical implications. This confirms that the subsequent introduction of H_2 did not alter reservoir permeability. This is a key finding, as it indicates that hydrogen injection does not induce measurable changes in reservoir flow properties under the investigated conditions. The preservation of permeability is critical for maintaining injectivity and withdrawal performance over repeated storage cycles, supporting the long-term operational viability of UHS in depleted gas reservoirs.

In addition to pressure and permeability behaviour, the thermal evolution of the reservoir provides an important perspective on system performance. The subsurface temperature trends observed during both storage cycles, shown in Fig. 5, offer insight into the thermal dynamics of the reservoir under H_2 injection and withdrawal conditions.

During injection phases, a slight decrease in reservoir temperature was recorded, which reflects the cooling effect of H_2 introduced at a lower temperature than the native formation. This behaviour is consistent with gas injection into porous media, where thermal equilibration is governed by the heat capacity and conductivity of the surrounding rock matrix [58]. The limited magnitude of cooling indicates efficient heat exchange with the formation, reducing the risk of thermal gradients that could affect reservoir properties or well integrity.

In stationary phases, such as those depicted in Fig. 5, the reservoir temperature stabilized between 33 °C and 34 °C, reflecting equilibrium conditions. This plateau suggests that thermal recovery occurs relatively quickly once injection ceases, maintaining a stable baseline in the absence of active flow. This return to equilibrium suggests strong thermal buffering by the reservoir, which is important for maintaining stable operating conditions during cyclic storage.

During withdrawal, a modest increase of up to 0.5 °C above the baseline was observed, likely reflecting the extraction of warmer gas from the reservoir. This limited thermal response indicates that thermal perturbations remain localized and do not significantly impact reservoir conditions, further supporting the stability of the system during cyclic operation.

A temporary temperature offset (<1 °C) observed between November 2023 and October 2024 was attributed to sensor drift, which was confirmed by the return to baseline conditions following gauge replacement. This demonstrates the importance of instrumentation reliability and validation in interpreting subsurface monitoring data. In summary, the temperature data confirm that the reservoir responds predictably to thermal perturbations associated with H_2 cycling, demonstrating strong thermal resilience of the formation. The absence of significant temperature fluctuations or persistent thermal gradients suggests that thermal effects are unlikely to impact reservoir performance, material integrity, or operational stability under the investigated conditions.

Together, the stable pressure response, unchanged permeability, and limited thermal effects provide strong evidence that the subsurface system remained mechanically and thermally stable under hydrogen storage conditions, supporting the feasibility of repeated and long-term UHS operation.

3.3. Microbiological analysis of subsurface brine

Microbial dynamics were monitored at the Rubensdorf demonstrator site using 16S rRNA gene amplicon sequencing. To assess potential microbiological changes associated with H_2 exposure, samples were also collected prior to hydrogen injection (2018–2021). Hydrogenotrophic methanogens dominated the reservoir community, as shown in Fig. 6. The relative abundance of hydrogenotrophic methanogens remained stable throughout the study period; however, the dominant methanogenic lineages shifted over time. In October 2018, the methanogenic signal was associated with two distinct Methanobacteriaceae lineages [59], whereas in February 2020, Methanocalculus [60] became the dominant hydrogenotrophic methanogen. By April 2021, hydrogenotrophic methanogens were nearly absent, but in March 2025, they returned to a state of high relative abundance, primarily represented by one unclassified Methanobacteriaceae lineage. Lineages

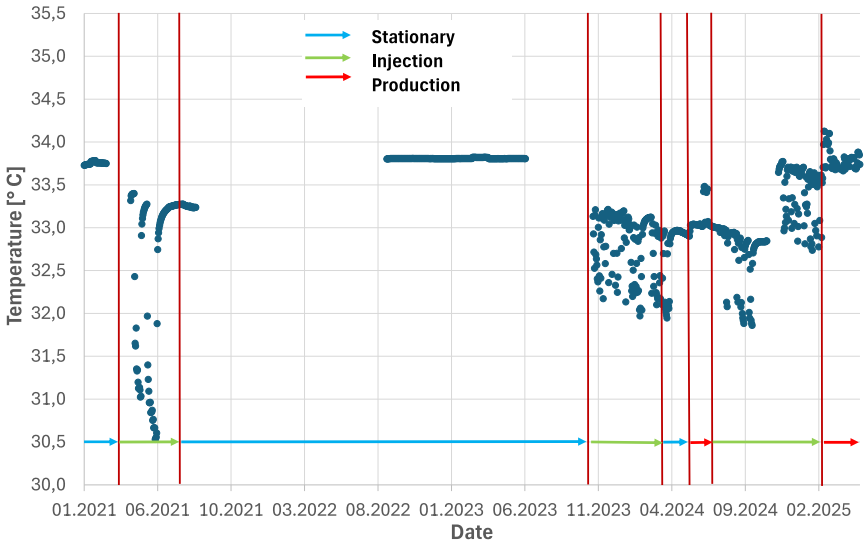

Fig. 5. Temperature profile during preparation and the two storage cycles in the Rubensdorf 2 A well. Red vertical lines indicate change of operation mode.

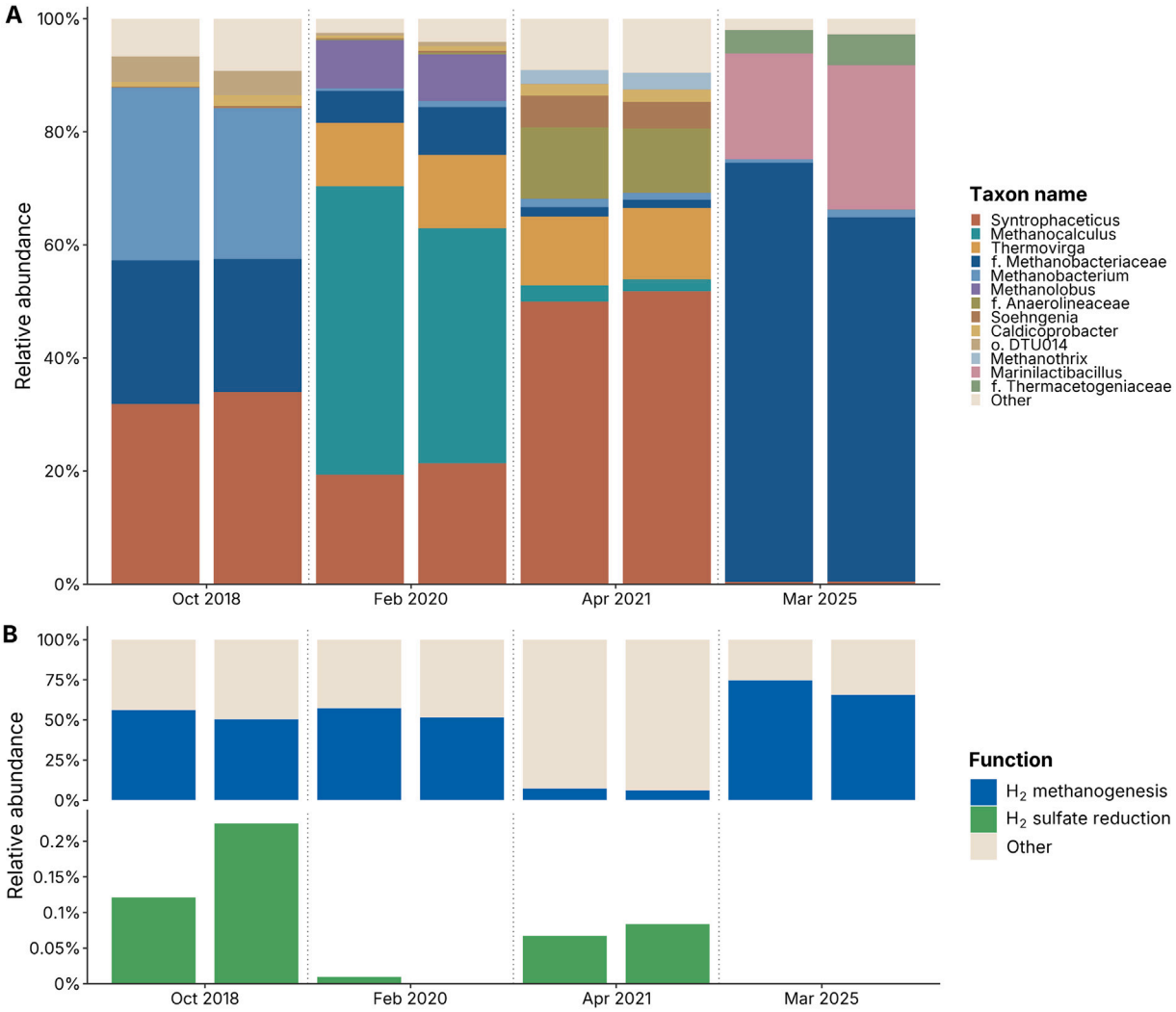

Fig. 6. Microbial community structure and H2-dependent functional potential at the Rubensdorf demonstrator. Panel A: genus-level relative abundance (16S rRNA, SILVA 138.2; genera < 2% pooled as "Other"). Panel B: FAPROTAX-inferred relative abundance of the two H_2-consuming guilds, hydrogenotrophic methanogenesis and hydrogenotrophic sulphate reduction (note the different *y*-axis scales).

Table 4
Selected biological and chemical parameters of Rubensdorf demonstrator.

	ATP [pg/mL]	DNA [ng/μL]	DOC [mg/L]	DIC [mg/L]	K^+ [mg/L]
Oct 2018	230	1.1	2810	139	n/a
Feb 2020	1251	30.1	1286	205	3200
April 2021	332	17.2	1522	225	1249
March 2025	6	2.9	31 052	8	8877

capable of sulphate reduction [31] remained very low throughout the study period and were not detected in the post-operational sampling in March 2025.

As shown in Table 4, ATP and DNA concentrations were comparable to active oil fields [61] during the first sampling in October 2018 and again during natural gas injection in April 2021. A temporary increase was observed in February 2020, after which levels declined markedly, reaching 6 pg/mL ATP, which is the level of measurement kit blank reading, and 2.9 ng/μ L DNA during H_2 withdrawal in March 2025. Dissolved Organic Carbon (DOC) and Potassium (K^+) exhibited relatively stable concentrations from 2018 to 2021 samples, whereas both parameters increased sharply in March 2025.

The dominance of hydrogenotrophic methanogens (Fig. 6) is consistent with their widespread occurrence in porous subsurface systems [28]. Their stable overall abundance indicates that hydrogen injection in late 2023 did not elicit a measurable functional response in the reservoir microbiome. The temporary decline in methanogens observed in April 2021 likely reflects operational influence [62] with the proportion of hydrogenotrophic methanogens returning to pre-injection levels by March 2025. Additionally, the elevated, yet still low ATP and DNA values in the February 2020 sample as seen in Table 4, most likely reflect transient microbial proliferation in stagnant borehole brine during a period of operational inactivity rather than in-situ reservoir activity. The disappearance of sulphate reducing lineages in March 2025 might also reflect specific operational conditions. Although in principle this sample should be the most representative of reservoir conditions because gas withdrawal draws brine from deeper within the formation and dilutes the sump with fresh brine, elevated dissolved organic carbon (DOC) and Potassium (K^+) values may indicate operational fluid contamination (proprietary liquid from operating company) associated with the October 2021 workover. Overall, these observations emphasize that operational context is essential for reliable chemical and microbiological brine characterization within routine reservoir monitoring and maintenance [62,63].

In summary, no enhanced microbial activity was observed after H_2 storage during the demonstration cycles at the Rubensdorf site. This conclusion is supported by lack of increase of ATP and DNA concentrations as well as stable relative abundances of hydrogenotrophic methanogens. These findings demonstrate that although native reservoir microbiota possess the metabolic potential to convert H_2 and CO_2 to methane and to reduce SO_4^{2-} to H_2S under suitable conditions, their activity is tightly constrained by the availability of electron acceptors such as CO_2 and SO_4^{2-} [64,65]. Under the current geochemical conditions at the Rubensdorf demonstrator site, the risk of H_2 loss or gas-quality degradation through microbial processes appears minimal. Nevertheless, the detection of minor microbial methane formation in controlled experiments highlights the importance of monitoring CO_2 dynamics, especially in future storage scenarios involving longer residence times or variable injection regimes. The need for an improved representative sampling approach for porous reservoirs became evident and should be a focus of future research [66].

3.4. Uncertainties and boundary conditions

3.4.1. Subsurface uncertainties and boundary conditions

A quantitative hydrogen mass balance was not conducted due to the inherent challenges of resolving gas distribution between working gas and cushion gas. In underground gas storage (UGS), mass balance closure at reservoir scale between working gas and cushion gas is generally not feasible, as mixing, dispersion, dissolution, and reservoir heterogeneity prevent precise accounting.

Injected and produced volumes were continuously monitored for regulatory purposes. However, these data alone are not sufficient to determine hydrogen recovery, as gas composition during withdrawal is governed by dynamic mixing processes with the cushion gas rather than by a simple volumetric balance. The observed concentration and pressure trends nevertheless indicate that hydrogen was predominantly recovered (with more than 98% purity) from the injected working gas volume, with only limited mixing with the cushion gas. A rigorous reservoir-scale hydrogen mass balance would require depletion of the storage system beyond normal operating conditions and was therefore outside the scope of this study.

To further support the interpretation of the observed field behaviour, numerical simulations of subsurface hydrogen transport are currently in an advanced stage of development. These include compositional flow modelling and analysis of key transport mechanisms such as relative permeability, dispersion, solubility, and diffusion, evaluated both individually and in coupled systems. A detailed evaluation will be presented in a forthcoming publication.

Furthermore, site-specific geomechanical analyses have not been conducted for the Rubensdorf field. However, studies from analogous UGS facilities in the Austrian Molasse Basin, demonstrate that clay- and shale-rich formations remain geomechanically stable under cyclic loading and unloading associated with pressure variations during gas storage operations [67]. As these processes are governed primarily by pressure changes rather than the composition of the stored gas, the findings are considered transferable to UHS conditions. In addition, recent studies on caprock stability in clay-rich lithologies of similar composition indicate that hydrogen exposure does not alter geomechanical properties [68,69], supporting the applicability of these findings to Molasse Basin formations.

In terms of biogeochemical processes, H_2S concentrations remained below DL throughout the withdrawal period, indicating limited biogeochemical reactivity under the investigated conditions. Consequently, detailed biogeochemical modelling was not prioritized within the scope of the present study. The present microbiological assessment is based on two hydrogen storage cycles and a comprehensive evaluation of long-term microbial stability will require extended operational periods. The functional interpretation is based on 16S rRNA gene amplicon data with FAPROTAX-based functional inference (Fig. 6). However, this approach reflects metabolic potential rather than realized activity. A conclusive assessment of functional stability would require measurements such as functional marker gene quantification (mcrA, dsrB), metagenomics or metatranscriptomics. Furthermore, the findings are considered transferable within the Molasse Basin due to the comparable geological setting. However, their applicability beyond the Molasse Basin is constrained by variations in reservoir properties, geochemistry, salinity or temperature. Additional uncertainty arises from sampling conditions, as well-sump brine collected may be influenced by operational artefacts [62], as indicated by elevated DOC and K+ in the March 2025 sample (Table 4).

3.4.2. Surface uncertainties and boundary conditions

The present study demonstrates that H_2 can be withdrawn from the UHS facility at purities of approximately 98%, thereby meeting the ISO 14687 Grade A specification for H_2 content without dedicated purification. While the H_2 concentration fullfils the standard requirement, compliance with all impurity limits has not yet been fully achieved. Nevertheless, the results indicate that full compliance may be within reach. A higher H_2 fraction in the cushion gas would reduce reservoir dilution and could further improve the quality of the recovered gas. Overall, the achievable product quality is reservoir-specific and depends on factors such as reservoir setting, cushion gas

composition and retention time. It must therefore always be assessed against the actual end-user purity requirements.

At present, H_2 quality requirements for emerging hydrogen infrastructure remain uncertain, as dedicated hydrogen pipeline networks are under development and quality specifications have not yet been fully harmonized across countries. More stringent purity specifications will increase overall storage costs, as a larger fraction of the withdrawn gas stream may require on-site purification. The use of pure H_2 as cushion gas could mitigate dilution effects and improve withdrawal purity, although its economic viability depends on the cost of hydrogen as cushion gas. The results of the current study indicate that a recovered H_2 purity of approximately 98% may represent a cost-efficient target specification for H_2-storage facilities. Whether higher purity requirements should be met through centralized purification at storage sites or decentralized purification at end-user facilities requires further evaluation.

While the current study supports the technical feasibility of UHS and does not indicate economically relevant H_2-losses, a comprehensive techno-economic assessment is still required to determine the trade-off between storage performance, hydrogen purity requirements, and the cost of gas conditioning. Planned future work will evaluate overall system efficiency, including compression and conditioning requirements (e.g., on the basis of the H_2-Optimum project [70]). Compared to natural gas storage, H_2 storage is expected to exhibit higher specific investment and operational costs per unit of energy because H_2 possesses only approximately one-third of the volumetric energy density of natural gas, requiring larger gas volumes to be handled for the same energy throughput.

4. Conclusions

This study demonstrates that depleted gas reservoirs represent a suitable and secure option for large-scale UHS. The demonstration-scale facility at Rubensdorf successfully achieved TRL 7 under real-field operating conditions. Across two storage cycles of pure H_2, a maximum stored volume of approximately 450 000 Nm^3 was reached, and the withdrawn H_2 consistently exceeded 98.0% purity prior to any surface conditioning. H_2S remained below the DL, and reservoir surveillance showed behaviour closely comparable to conventional natural gas storage, indicating preserved caprock integrity, stable reservoir performance and predictable cyclic operation. Over the two storage cycles studied, and under the geochemical conditions at Rubensdorf, there was no evidence of significant microbial H_2 consumption, and the risk of gas-quality degradation through microbial activity appears low. This reflects operational feasibility under the investigated conditions and indicates microbial stability over the two storage cycles investigated.

The results confirm that seasonal H_2 storage in porous formations can deliver a reliable H_2 supply at standardized purity. Two complementary purity-assurance strategies were validated: (1) using a H_2 cushion gas to limit reservoir dilution and achieve pipeline-grade H_2 (<98% purity), and (2) an on-site purification system for applications requiring higher purity specifications. Together, these approaches offer operational flexibility across diverse industrial and market contexts.

With increasing evidence from field demonstrations and decades of transferable expertise from natural gas storage, technical barriers to UHS are diminishing. Future large-scale deployment is expected to depend increasingly on the development of H_2 supply chains, regulatory frameworks and market structures.

From an economic perspective, an indicative service price of 30–40 €/MWh for UHS has been communicated publicly. Assuming that only 20%–25% of the annual turnover volume needs to be stored (similar to the natural gas market today), the hydrogen price would increase by 6–10 €/MWh or 0.25–0.40 €/kg for storage services [71,72].

Future work will continue within the EUH2STARS project [73], focusing on further operation of the Rubensdorf demonstrator facility and the implementation of a next-generation H_2 purification system. This system aims to process the full withdrawal stream and deliver two standardized product gases: pure H_2 and pipeline-specification natural gas, produced through a combined HPSA and membrane-permeation process [74]. These developments are expected to further strengthen the technological and economic foundation for large-scale UHS in porous formations.

CRediT authorship contribution statement

Anitha Andiappan: Writing – review & editing, Writing – original draft, Visualization, Validation, Supervision, Software, Methodology, Investigation, Formal analysis, Data curation, Conceptualization. **Franziska Steger:** Writing – review & editing, Validation, Supervision, Formal analysis, Conceptualization. **Aleksander Makaruk:** Writing – review & editing, Writing – original draft, Methodology, Formal analysis, Data curation. **Artur Zaduryan:** Writing – original draft, Methodology, Formal analysis, Data curation. **Katarina Nieke:** Writing – original draft, Methodology, Data curation. **Benedikt Hasibar:** Writing – review & editing. **Andreas P. Loibner:** Writing – review & editing, Supervision. **Markus Pichler:** Writing – review & editing, Writing – original draft, Supervision, Methodology. **Stephan Bauer:** Writing – review & editing, Writing – original draft, Supervision, Funding acquisition, Conceptualization.

Declaration of generative AI and AI-assisted technologies in the manuscript preparation process

During the preparation of this work the authors used Copilot in order to improve clarity and readability of the text. After using this tool, the authors reviewed and edited the content as needed and take full responsibility for the content of the published article.

Declaration of competing interest

The authors declare the following financial interests/personal relationships which may be considered as potential competing interests: Aleksander Makaruk, Benedikt Hasibar, Markus Pichler, Stephan Bauer has patent Method For Operating Gas Storage Devices, And Device For Carrying Out The Methods issued to AXIOM GmbH & RAG Austria AG. Stephan Bauer, Markus Pichler, Benedikt Hasibar, Anitha Andiappan has patent METHOD FOR OPERATING GAS DEPOSITS AND GAS RESERVOIRS issued to RAG Austria AG. The authors AA, FS, KN, BH, MP and SB are employees of RAG Austria AG, which is engaged on this and other projects involving Underground Hydrogen Storage. (UHS) If there are other authors, they declare that they have no known competing financial interests or personal relationships that could have appeared to influence the work reported in this paper.

Acknowledgments

Funding: The authors gratefully acknowledge the financial support provided by the Austrian Climate and Energy Fund and the Austrian Research Promotion Agency (FFG) for the flagship project USS2030 (www.uss-2030.at, FFG project no. 880764) as well as by the Clean Hydrogen Partnership and the European Union for the flagship project EUH2STARS (www.euh2stars.eu, Grant agreement ID: 101137798) which form the basis of this publication. The CAPEX costs primarily for the electrolyzer and the gas compressor, were partly funded by Kommunalkredit Public Consulting (KPC proposal no. C062754)

Appendix A. Supplementary data

Supplementary material related to this article can be found online at https://doi.org/10.1016/j.ijhydene.2026.156784.

References

[1] Oyenuga MO, Singh R, Apata SB, Khan S, Kumar V. Energy transition: Fossil fuels versus renewables. In: Smart technologies for climate change and net zero policies: practical approaches towards sustainability. Cham: Springer Nature Switzerland; 2025, p. 123–30. http://dx.doi.org/10.1007/978-3-031-92221-3_20.

[2] Enasel E, Dumitrascu G. Storage solutions for renewable energy: A review. Energy Nexus 2025;17:100391. http://dx.doi.org/10.1016/j.nexus.2025.100391.

[3] Elazab M, Elgohr AT, Bassyouni M, Kabeel AE, Attia MEH, Elshaarawy MK, Hamed AK, Alzahrani HA. Green hydrogen: Unleashing the potential for sustainable energy generation. Results Eng 2025;27:106031. http://dx.doi.org/10.1016/j.rineng.2025.106031.

[4] Patonia A, Lambert M, Lin N, Shuster M. Underground storage for decarbonisation: Trade-offs between hydrogen, natural gas, and carbon dioxide. Energy Transition Report ET47, Oxford: Oxford Institute for Energy Studies; 2025, URL https://www.oxfordenergy.org/wpcms/wp-content/uploads/2025/06/ET47-Underground-storage-for-decarbonisation.pdf. [Accessed 31 October 2025].

[5] Burke A, Ogden J, Fulton L, Cerniauskas S. Hydrogen storage and transport: Technologies and costs. Tech. rep. UCD-ITS-RR-24-17, California: Institute of Transportation Studies, University of California, Davis; 2024, URL https://escholarship.org/content/qt83p5k54m/qt83p5k54m_noSplash_8bb1326c13cfb9aa3d0d376ec26d3e06.pdf. [Accessed 31 October 2025].

[6] Artelys and Frontier Economics. Why European underground hydrogen storage needs should be fulfilled. Tech. rep., Brussels: Gas Infrastructure Europe (GIE); 2024, URL https://www.gie.eu/wp-content/uploads/filr/9697/RPT-EU_Underground_Hydrogen_Storage_Targets-090424-CLEAN.pdf. [Accessed 31 October 2025].

[7] BMK. Wasserstoffstrategie für Österreich. Tech. rep., Wien: Bundesministerium für Klimaschutz, Umwelt, Energie, Mobilität, Innovation und Technologie (BMK); 2022, URL https://www.bmwet.gv.at/Services/Publikationen/publikationen-energie/wasserstoffstrategie.html. [Accessed 02 January 2026].

[8] Federal Ministry for Economic Affairs and Climate Action (BMWK). National hydrogen strategy. 2023, URL https://www.bundeswirtschaftsministerium.de/Redaktion/EN/Hydrogen/Dossiers/national-hydrogen-strategy.html. [Accessed 15 December 2025].

[9] Nationaal Waterstofprogramma. National hydrogen strategy Netherlands. 2023, URL https://www.nationaalwaterstofprogramma.nl/documenten/handlerdownloadfiles.ashx?idnv=2379389. [Accessed 15 December 2025].

[10] France Hydrogène. National hydrogen strategy France. 2023, URL https://www.france-hydrogene.org/app/uploads/sites/4/2023/10/France-Hydrogene_National-Hydrogen-Strategy_EN.pdf. [Accessed 15 December 2025].

[11] UK Government. Hydrogen net zero investment roadmap. 2023, URL https://www.gov.uk/government/publications/hydrogen-net-zero-investment-roadmap. [Accessed 15 December 2025].

[12] Baumann M, Felber B, Reuter S, Orsolits D, Siebenhofer D, Wallner S, Stangl F, Fliedl M. Wasserstoffspeicher in Österreich. Studie, Wien: Österreichische Energieagentur – Austrian Energy Agency; 2025, URL https://www.bmwet.gv.at/dam/jcr:b8f68e4d-ac2d-4175-a0fc-84b64a803e44/Wasserstoffspeicher%20in%20%C3%96sterreich.pdf. [Accessed 02 January 2026].

[13] Ruhnau O, Qvist S. Storage requirements in a 100% renewable electricity system: extreme events and inter-annual variability. Environ Res Lett 2022;17(4):044018. http://dx.doi.org/10.1088/1748-9326/ac4dc8.

[14] Uliasz-Misiak B, Misiak J. Underground gas storage in saline aquifers: Geological aspects. Energies 2024;17:1666. http://dx.doi.org/10.3390/en17071666.

[15] CEDIGAZ. Underground gas storage in the world – 2023 status. Tech. rep., Rueil-Malmaison, France: CEDIGAZ; 2024, URL https://www.cedigaz.org/underground-gas-storage-in-the-world-2023-status/. [Accessed 31 October 2025].

[16] Groß T, Dunkel P, Linßen J, Stolten D. EU-scale hydrogen system scenarios. Tech. rep., HyUSPRe Project; 2024, URL https://www.hyuspre.eu/wp-content/uploads/2024/06/WP7_D7.2_EU-scale-hydrogen-system-scenarios_2024.06.27.pdf. HyUSPRe Deliverable D7.2. [Accessed 02 January 2026].

[17] Michalski J, Zerhusen J, Bünger U. Expected techno-economic requirements for underground renewable hydrogen storage. Tech. rep., Ludwig-Bölkow-Systemtechnik GmbH; 2021, URL https://hystories.eu/wp-content/uploads/2021/05/D5.2_Hystories_Storage_requirements.pdf. HyStories Deliverable D5.2. [Accessed 02 January 2026].

[18] Edlmann K, Hemming C, Dopffel N, Groenenberg R, van Gessel S, Andiappan A, Pichler M, Hogeweg S, Kosack C, Strobel G, Lenze A, Lesche C, Westhues A, Réveillère A, Mclane C, Stevenson R. Underground hydrogen storage: From field insights to commercial deployment. 2025, Submitted to Nature Reviews Earth & Environment.

[19] HyStorIES – hydrogen storage in European subsurface. 2021, URL https://hystories.eu/. [Accessed 02 January 2026].

[20] HyStorPor Project. HyStorPor project: Hydrogen storage in porous media. 2020, URL https://www.research.ed.ac.uk/en/projects/hystorpor-project/. [Accessed 20 November 2025]. University of Edinburgh Research Portal.

[21] HyUSPRe Project. HyUSPRe: Hydrogen underground storage in porous reservoirs. 2023, URL https://www.hyuspre.eu/. Project duration: 2023-2027. [Accessed 06 November 2025]. Horizon Europe Project.

[22] RAG Austria AG. Underground Sun Storage: Chemical storage of renewable energy in porous subsurface reservoirs with exemplary testbed. Final report, Vienna, Austria: RAG Austria AG; 2017, URL https://www.rag-austria.at/innovation/innovationsprojekte/underground-sun-storage. [Accessed 02 January 2026].

[23] RAG Austria AG. Underground Sun Conversion: Renewable energy storage and conversion by in-situ biological methanation in porous underground gas reservoirs. Final report, Vienna, Austria: RAG Austria AG; 2023, URL https://www.rag-austria.at/innovation/innovationsprojekte/underground-sun-conversion. [Accessed 02 January 2026].

[24] Bensing JP, Misch D, Andiappan A, Pichler M. Gas exposure trials of the hall formation, lehen field, Austria: Laboratory simulations of gas-caprock-brine interactions in an underground hydrogen storage system. Int J Hydrog Energy 2024;90:1100–11. http://dx.doi.org/10.1016/j.ijhydene.2024.10.067.

[25] Bauer S, Pichler M. Underground Sun Storage: Ein Projekt zur Erforschung der Wasserstoffverträglichkeit von Erdgasporenspeichern. 2017, URL https://www.dvgw.de/medien/dvgw/forschung/berichte/1708bauer.pdf. DVGW Forschungsbericht. [Accessed 20 November 2025].

[26] Andiappan A, Pichler M, Bauer S. Investigation of subsurface integrity of depleted porous gas reservoirs for the purpose of hydrogen storage. In: SPE europec featured at EAGE conference and exhibition. Vienna, Austria; 2023, http://dx.doi.org/10.2118/214432-MS.

[27] Michelsen J, Hagemann B, Ganzer L, Pichler M, Andiappan A. Mechanical dispersion in UHS: Insights from laboratory experiments on hydrogen-methane interactions. In: DGMK/ÖGEW Frühjahrstagung 2024. 2024, URL https://dgmk.de/app/uploads/2024/04/A-139_Michelsen.pdf. [Accessed 02 January 2026].

[28] Dopffel N, Jansen S, Gerritse J. Microbial side effects of underground hydrogen storage—Knowledge gaps, risks and opportunities for successful implementation. Int J Hydrog Energy 2021;46(12):8594–606. http://dx.doi.org/10.1016/j.ijhydene.2020.12.058.

[29] Wu L, Hou Z-M, Luo Z-F, Fang Y-L, Huang L-C, Wu X-N, Chen Q-J, Wang Q-C. Impacts of microbial interactions on underground hydrogen storage in porous media: A comprehensive review of experimental, numerical, and field studies. Pet Sci 2024;21(6):4067–99. http://dx.doi.org/10.1016/j.petsci.2024.08.015.

[30] Xiong Z, Hou J, Du Q, Chen Z, Lu X, Liu Y, Wei B, Lu T. A comprehensive review of H_2 physical behavior and H_2-rock-microbial interactions in underground hydrogen storage. Energy 2025;326:136226. http://dx.doi.org/10.1016/j.energy.2025.136226.

[31] Muyzer G, Stams AJM. The ecology and biotechnology of sulphate-reducing bacteria. Nat Rev Microbiol 2008;6(6):441–54. http://dx.doi.org/10.1038/nrmicro1892.

[32] Vahabzadeh E, Hogeweg S, Nazari F, Hagemann B, Polya DA, Lloyd JR, Niasar V. Evaluating hydrogen loss in underground storage: The role of microbial activity, mixing, and operational strategies. Energy Fuels 2025;39(37). http://dx.doi.org/10.1021/acs.energyfuels.5c02352.

[33] Hasibar B, Pichler M. In: Hasibar B, Sidler D, editors. Underground Sun Conversion – Flexible Storage (USC-FlexStore): Final Report. Final report, Vienna and Bern: RAG Austria AG and Energie 360° AG; 2023, URL https://www.rag-austria.at/innovation/innovationsprojekte/usc-flexstore. Chapter 3.

[34] ISO 14687:2025 — Hydrogen fuel quality — product specification. 2025, URL https://www.iso.org/standard/82660.html. Second Edition.

[35] Polman EA, Doelman ML, van Greuningen S, Turkstra JW, van Essen M, Vlap H. A follow-up study into the hydrogen quality requirements. Tech. rep., Kiwa Technology B.V. and DNV; 2023, URL https://www.eerstekamer.nl/nonav/overig/20231009/rapport_kiwa_dnv/document. [Accessed 02 January 2026].

[36] Covault JA, Graham SA. Turbidite architecture in proximal foreland basin-system deep-water depocenters: insights from the tertiary of western europe. Austrian J Earth Sci 2008;101:36–51, URL https://www.zobodat.at/pdf/MittGeolGes_101_0036-0051.pdf. [Accessed 31 October 2025].

[37] Polesny H. Stratigraphy and hydrocarbons in the molasse foredeep of upper Austria and Salzburg. In: Field guide: transect through central eastern alps. Vienna, Austria: Carpathian-Balkan Geological Association, XVI Congress; 1998, p. 25–36, URL https://opac.geologie.ac.at/ais312/dokumente/OEMG_Band_144_1999.pdf. [Accessed 31 October 2025].

[38] Veron J. The Alpine molasse basin – review of petroleum geology and remaining potential. Bull Angew Geol 2005;10(1):75–86.

[39] Gier S. Diagenese peltischer Sedimente in der Molassezone Oberösterreichs. Mitt Österr Miner Ges 1999;144:45–68, URL https://opac.geologie.ac.at/ais312/dokumente/OEMG_Band_144_1999.pdf. [Accessed 31 October 2025].

[40] Truschner M, Trautmann A, Mori G. The basics of hydrogen uptake in iron and steel. BHM Berg- Hüttenmänn Monatsh. 2021;166(9):443–9. http://dx.doi.org/10.1007/s00501-021-01142-x.

[41] Kuloglija S, Kolur NA, Kalman V, Jordan C, Golda M, Makaruk A, Engin E, Balla A, Harasek M. Hydrogen purification from underground storage via pressurized adsorption: Impact of adsorbent properties and operating parameters on methane separation. Int J Hydrog Energy 2025;136:402–12. http://dx.doi.org/10.1016/j.ijhydene.2025.05.090.

[42] Kalman V, Makaruk A, Engin E, Balla A, Harasek M. Simulation of hydrogen-methane separation with pressure swing adsorption. In: Computer aided chemical engineering. Elsevier; 2024, p. 931–6. http://dx.doi.org/10.1016/B978-0-443-28824-1.50156-3.

[43] Sam G, Kaestenbauer M, Burgstaller C, Chevelcha E. Fully automated fluid level measurement tool. In: SPE Asia Pacific oil and gas conference and exhibition, no. SPE-145434, Jakarta, Indonesia: Society of Petroleum Engineers; 2011, Affiliations: RAG Austria; SPE; Mining University Leoben.

[44] Burgstaller C. New approaches of using fluid level data for production optimization and reservoir engineering applications. In: SPE europec at the 78th EAGE conference and exhibition, no. SPE-180159-MS, Vienna, Austria: Society of Petroleum Engineers; 2016, Affiliation: RAG Austria. Presented 30 May–2 June 2016..

[45] Hellerschmied C, Schritter J, Waldmann N, Zaduryan AB, Rachbauer L, Scherr KE, Andiappan A, Bauer S, Pichler M, Loibner AP. Hydrogen storage and geo-methanation in a depleted underground hydrocarbon reservoir. Nat Energy 2024;9(3):333–44. http://dx.doi.org/10.1038/s41560-024-01458-1.

[46] Parada A, Needham D, Fuhrman J. Every base matters: assessing small subunit rRNA primers for marine microbiomes with mock communities, time series and global field samples. Environ Microbiol 2016;18(5):1403–14. http://dx.doi.org/10.1111/1462-2920.13023.

[47] Apprill A, McNally S, Parsons R, Weber L. Minor revision to V4 region SSU rRNA 806R gene primer greatly increases detection of SAR11 bacterioplankton. Aquat Microb Ecol 2015;75(2):129–37. http://dx.doi.org/10.3354/ame01753.

[48] Quast C, Pruesse E, Yilmaz P, Gerken J, Schweer T, Yarza P, Peplies J, Glöckner F. The SILVA ribosomal RNA gene database project: improved data processing and web-based tools. Nucleic Acids Res 2013;41(D1):D590–6. http://dx.doi.org/10.1093/nar/gks1219.

[49] Callahan BJ, McMurdie PJ, Rosen MJ, Han AW, Johnson AJA, Holmes SP. DADA2: High-resolution sample inference from illumina amplicon data. Nature Methods 2016;13:581–3. http://dx.doi.org/10.1038/nmeth.3869.

[50] Louca S, Parfrey LW, Doebeli M. Decoupling function and taxonomy in the global ocean microbiome. Science 2016;353(6305):1272–7. http://dx.doi.org/10.1126/science.aaf4507.

[51] Kumar A, Kimbler OK. The effect of mixing and gravitational segregation between natural gas and inert cushion gas on the recovery of gas from horizontal storage aquifers. In: Northern plains section regional meeting of the society of petroleum engineers of AIME. Omaha, Nebraska, USA: Society of Petroleum Engineers (SPE); 1972, SPE-3866-MS.

[52] Bachu S, Bennion B. Effects of in-situ conditions on relative permeability characteristics of CO_2-brine systems. Environ Geol 2008;54:1707–22. http://dx.doi.org/10.1007/s00254-007-0946-9.

[53] Mawa K, Fernandes BRB, Delshad M, Lake LW, Sepehrnoori K. Dispersion during underground hydrogen storage in depleted gas reservoirs. Clean Energy Sustain 2026;4(2):10009. http://dx.doi.org/10.70322/ces.2026.10009.

[54] Lu J, Muhammed NS, Okolie JA, Epelle EI. A sensitivity study of hydrogen mixing with cushion gases for effective storage in porous media. Sustain Energy Fuels 2025;9(5):1353–70. http://dx.doi.org/10.1039/D4SE01400F.

[55] Spycher N, Pruess K, Ennis-King J. CO_2–H_2O mixtures in the geological sequestration of CO_2. I. Assessment and calculation of mutual solubilities from 12 to 100 °C and up to 600 bar. Geochim Cosmochim Acta 2003;67(16):3015–31. http://dx.doi.org/10.1016/S0016-7037(03)00273-4.

[56] Duan Z, Sun R. An improved model calculating CO_2 solubility in pure water and aqueous NaCl solutions from 273 to 533 K and from 0 to 2000 bar. Chem Geol 2003;193(3–4):257–71. http://dx.doi.org/10.1016/S0009-2541(02)00263-2.

[57] Greiml M, Bauer S, Bogner W, Makaruk A, Pichler M, Sachsenhofer M, Sam G, Strasser F. Measurement monitoring and verification plan of RAG's Rubensdorf site. Tech. Rep. D2.1, Vienna: EUH2STARS Consortium; 2024, URL https://www.euh2stars.eu/en/publications/project-results. [Accessed 02 January 2026].

[58] Yang Y, Zandanel A, Liu S, Neil CW, Germann TC, Gross MR. Temperature dependence of hydrogen diffusion in reservoir rocks: implications for hydrogen geologic storage. Energy Adv 2024;3(8):2051–65. http://dx.doi.org/10.1039/D4YA00233D.

[59] Boone DR. Methanobacterium. In: Trujillo ME, Dedysh S, DeVos P, Hedlund B, Kämpfer P, Rainey FA, Whitman WB, editors. Bergey's manual of systematics of archaea and bacteria. John Wiley & Sons; 2015, http://dx.doi.org/10.1002/9781118960608.gbm00495.

[60] Ollivier B, Fardeau M-L, Cayol J-L, Magot M, Patel BKC, Prensier G, Garcia J-L. Methanocalculus halotolerans gen. nov., sp. nov., isolated from an oil-producing well. Int J Syst Bacteriol 1998;48(3):821–8. http://dx.doi.org/10.1099/00207713-48-3-821.

[61] Jones LM, Hanrahan N, Salta M, Skovhus TL, Thomas K, Illson T, Wharton J, Webb JS. Toward simulating offshore oilfield conditions: insights into microbiologically influenced corrosion from a dual anaerobic biofilm reactor. Appl Environ Microbiol 2025;91:e02221–24. http://dx.doi.org/10.1128/AEM.02221-24.

[62] Zaduryan A, Pichler M, Waldmann N, Riedl C, Müllern K, Hasibar B, Loibner A. An in-situ biosampling device for separating reservoir-associated from wellbore-specific microbial signals in underground gas reservoirs. Int J Hydrog Energy 2026;212(153521). http://dx.doi.org/10.1016/j.ijhydene.2026.153521.

[63] Wilkins MJ, Daly RA, Mouser PJ, Trexler R, Sharma S, Cole DR, Wrighton KC, Biddle JF, Denis EH, Fredrickson JK, Kieft TL, Onstott TC, Peterson L, Pfiffner SM, Phelps TJ, Schrenk MO. Trends and future challenges in sampling the deep terrestrial biosphere. Front Microbiol 2014;5:481. http://dx.doi.org/10.3389/fmicb.2014.00481.

[64] Thaysen EM, McMahon S, Strobel GJ, Butler IB, Ngwenya BT, Heinemann N, Wilkinson M, Hassanpouryouzband A, McDermott CI, Edlmann K. Estimating microbial growth and hydrogen consumption in hydrogen storage in porous media. Renew Sustain Energy Rev 2021;151:111481. http://dx.doi.org/10.1016/j.rser.2021.111481.

[65] Dopffel N, Compassi L, Heydolph B, Kedir A, An-Stepec BA, Badstöber J, Boiadjieva-Scherzer T. Hydrogen competition between a gas reservoir community indicates available CO_2 as main limiting factor. FEMS Microbiol Lett 2026;373:fnag031. http://dx.doi.org/10.1093/femsle/fnag031.

[66] HYDRA Project. Hydrogen economy benefits and risks: tools development and policies implementation to mitigate possible climate impacts. 2023, URL https://www.hydraproject.eu/. Project duration: 2023-2027. [Accessed 06 November 2025]. Horizon Europe Project No. 101137758.

[67] INA d. Exploration & production laboratory. 2024, URL https://www.ina.hr/en/about-ina/core-business/exploration-and-production/explorationproduction-laboratory/. [Accessed 3 July 2026]. INA Corporate Website.

[68] Iyare UC, Zandanel A, Neil CW, C. BK, Rock M, Li W, Frash LP, Currier RP, German T, Gross MR. Impact of hydrogen exposure on the integrity of shale caprock for underground hydrogen storage. Int J Hydrog Energy 2025;161:150706. http://dx.doi.org/10.1016/j.ijhydene.2025.150706.

[69] Kumar KR. Geomechanical study of underground hydrogen storage (Ph.D. thesis), Delft University of Technology; 2023, http://dx.doi.org/10.4233/uuid:b3d264ce-e7dc-4e67-b0e1-94f3cc7831ca.

[70] DVGW. H2-Optimum I. 2024, URL https://www.dvgw.de/themen/forschung-und-innovation/forschungsprojekte/dvgw-forschungsprojekt-h2-optimum. [Accessed 3 July 2026]. DVGW Forschungsprojekt.

[71] Energate Messenger. Geologische Wasserstoffspeicher bereit zur Skalierung. 2025, URL https://www.energate-messenger.de/news/253118/geologische-wasserstoffspeicher-bereit-zur-skalierung. [Accessed 27 January 2026].

[72] RAG Austria AG. Erster Preisindikator für geologische Wasserstoffspeicherung. 2025, URL https://www.uss-2030.at/news/erster-preisindikator-fuer-geologische-wasserstoffspeicherung. [Accessed 27 January 2026].

[73] EUH2STARS Consortium. EUH2STARS – European Underground Hydrogen Storage Reference System. 2024, URL https://www.euh2stars.eu/en/. [Accessed 27 January 2026].

[74] Makaruk A, Bauer S, Pichler M, Hasibar B. Method for operating gas storage devices, and device for carrying out the method. 2025, URL https://worldwide.espacenet.com/publicationDetails/biblio?II=1&ND=3&adjacent=true&locale=de_EP&FT=D&date=20250918&CC=WO&NR=2025190750A1&KC=A1#. Filing date: 2025-09-18. Applicant: Axiom Angewandte Prozesstechnik Ges.m.b.H. and RAG Austria AG. Patent WO2025190750 A1.